Pediatric Neurology 94 (2019) 64–69

Contents lists available at ScienceDirect

Pediatric Neurology

journal homepage: www.elsevier.com/locate/pnu

Clinical Observations

Arrest of Fetal Brain Development in ALG11-Congenital Disorder of Glycosylation

Sarah B. Mulkey, MD, PhD [a, b, c, *], Bobby G. Ng, BS [d], Gilbert L. Vezina, MD [e], Dorothy I. Bulas, MD [e], Lynne A. Wolfe, MS, CRNP [f], Hudson H. Freeze, PhD [d], Carlos R. Ferreira, MD [f]

[a] Division of Fetal and Transitional Medicine, Children's National Health System, Washington, District of Columbia
[b] Department of Pediatrics, The George Washington University School of Medicine and Health Sciences, Washington, District of Columbia
[c] Department of Neurology, The George Washington University School of Medicine and Health Sciences, Washington, District of Columbia
[d] Human Genetics Program, Sanford Burnham Prebys Medical Discovery Institute, La Jolla, California
[e] Division of Radiology, Children's National Health System, Washington, District of Columbia
[f] National Human Genome Research Institute, National Institutes of Health, Bethesda, Maryland

ARTICLE INFO

Article history:
Received 29 October 2018
Accepted 18 December 2018
Available online 24 December 2018

Keywords:
Congenital disorder of glycosylation
Fetal brain disruption sequence
Congenital microcephaly
Fetal magnetic resonance imaging

ABSTRACT

Background: Arrest of fetal brain development and the fetal brain disruption sequence describe a severe phenotype involving microcephaly, occipital bone prominence, and scalp rugae. Congenital disorders of glycosylation are a heterogeneous group of inherited disorders involved in glycoprotein and glycolipid biosynthesis, which can cause microcephaly and severe neurodevelopmental disability.
Methods: We report an example of fetal microcephaly diagnosed at 36 weeks' gestation with a history of normal fetal biometry at 20 weeks' gestation. Postnatal genetic testing was performed.
Results: Fetal magnetic resonance imaging at 36 weeks' gestational age showed severe cortical thinning with a simplified gyral pattern for gestational age, ventriculomegaly, and agenesis of the corpus callosum. The fetal skull had a posterior shelf at the level of the lambdoid suture, characteristic of fetal brain disruption sequence. Postnatal brain magnetic resonance imaging found no brain growth during the interval from the fetal to postnatal study. The infant was found to have biallelic pathologic mutations in *ALG11*.
Conclusions: Arrest of fetal brain development, with image findings consistent with fetal brain disruption sequence, is a previously unreported phenotype of congenital microcephaly in ALG11-congenital disorder of glycosylation. ALG11-congenital disorder of glycosylation should be considered in the differential diagnosis of this rare form of congenital microcephaly.

Introduction

Fetal brain disruption sequence is a severe neurological phenotype consisting of microcephaly, occipital bone prominence, and scalp rugae.[1] In congenital microcephaly resulting from fetal brain disruption sequence, the mechanism of the skull collapse is thought to result from decreased intracranial hydrostatic pressure associated with a disruption or "arrest" of brain growth usually in the second or third trimester when the fetal brain volume normally has significant increase.[1,2] This phenotype occurs from congenital infections including Zika virus,[3] fetal cerebral injury from vascular insults or maternal trauma, and in genetic conditions.[4] A similar term, "fetal brain arrest" has been proposed to refer to causes not associated with brain injury or infection, but which are felt to result from a genetic mutation.[4]

Congenital disorders of glycosylation (CDG) are a heterogeneous group of monogenic disorders involved in glycoprotein and glycolipid biosynthesis.[5,6] Affected infants have multisystemic abnormalities and often have neurological phenotypes, which include microcephaly, seizures, hypotonia, cerebellar hypoplasia, and severe intellectual disability.[7,8] ALG11-CDG results from a deficiency of guanosine diphosphate-mannose, $Man_3GlcNAc_2$-PP-dolichol/$Man_4GlcNAc_2$-PP-dolichol α-1,2-mannosyltransferase, the enzyme

Conflict of interest: The authors declare no conflict of interest.
URLs: gnomAD, http://gnomad.broadinstitute.org.

* Communications should be addressed to: Dr. Mulkey; Division of Fetal and Transitional Medicine; Children's National Health System; 111 Michigan Avenue, NW; Washington, DC 20010.
E-mail address: sbmulkey@childrensnational.org (S.B. Mulkey).

https://doi.org/10.1016/j.pediatrneurol.2018.12.009
0887-8994/

TABLE.
Clinical Features, Mutations, and Brain MRI Findings in 11 Reported Cases of ALG11-CDG

Clinical Feature	Rind et al., 2010[10] (Pt 1)	Rind et al., 2010[10] (Pt 2)	Thiel et al., 2012[11] (Pt 1)	Thiel et al., 2012[11] (Pt 2)	Thiel et al., 2012[11] (Pt 3)	Regal et al., 2015[12] (Pt 1)	Regal et al., 2015[12] (Pt 2)	Al Teneiji et al., 2017[13] (Pt 1)	Al Teneiji et al., 2017[13] (Pt 2)	Pereira et al., 2017[14]	Present Report
Age at presentation	1 week	6 weeks	Infancy	Infancy	Infancy	Birth at term	Age 3 months	Age 4 months	Age 4 months	Early life	Fetal, 36 weeks' gestation
Gender	Female*	Male*	Female	Female	Male	Male	Male	Female	Female	Female	Male
Microcephaly	+	NA	+	NA	−	+	+	+	+	+	+
Epilepsy	+	+	+	+	+	+	+	+	+	+	−
Hypotonia	Axial	+	Axial	Axial	Axial	Axial	Axial	+	+	+	+
Hypertonia	−	−	NA	NA	NA	Peripheral	Peripheral	NA	NA	NA	−
Global developmental delay	+	+	+	+	+	+	+	+	+	+	+
Eye/visual problems	+	NA	+	+	+	+	+	+	+	NA	+
Feeding problems	+	+	−	−	+	+	−	+	−	−	+
Outcome	Died at 2 years	NA	Alive at 7 years	Alive at 4.5 years	Alive at 8.5 years	Died at 3 years	Died at 4 months	Alive at 7 years	Alive at 4 years	Alive at 6 years	Alive at 20 months
Mutations: cDNA (NM_001004127.2)/ protein	hmz c.257T>C/ p.L86S	hmz c.257T>C/ p.L86S	c.623_642del/ p.S208Yfs*4; c.836A>C/ p.Y279S	c.1142T>C/ p.L381S; c.1192G>A/ p.E398K	hmz c.953A>C/ p.Q318P	c.479G>T/ p.G160V; c.45-2A>T	c.479G>T/ p.G160V; c.36dupG/ p.L13Vfs*44	hmz c.1241T>A/ p.I414N	hmz c.1123_ 1126delAACA/ p.N375Ffs*6	NA	c.44G>C/p.R15T; c.161C>T/p.S54L
Brain MRI	NA	NA	Cerebral atrophy and abnormal white matter	NA	NA	Cerebral atrophy, subcortical heterotopia, delayed myelination, simplified gyral pattern	Cerebral atrophy	Hypomyelination, brain atrophy, thin corpus callosum	Cerebral atrophy	Enlarged subarachnoid spaces; normal myelination and posterior fossa	Arrest of brain growth, agenesis of the corpus callosum, simplified gyral pattern
Other features	Temperature instability, deafness, inverted nipples, abnormal fat pads	Deafness		Oscillations of body temperature, inverted nipples		Sloping forehead, micrognathia	Burst suppression EEG, cochlear hearing loss	Inverted nipples, abnormal fat distribution		Epileptic spasms at age 5 months	Nonepileptic breath-holding episodes, inverted nipples

Abbreviations:
CDG = congenital disorders of glycosylation
EEG = electroencephalograph
hmz = homozygous
MRI = magnetic resonance imaging
NA = not available
+ = Present
− = Absent
* Siblings.

that catalyzes the addition of the fourth and fifth mannoses to the oligosaccharide precursor.[9] It was first described in a patient in 2010 with neurocognitive delays and epilepsy (Table).[10] The phenotype of ALG11-CDG was further characterized as severe psychomotor disability, progressive microcephaly, and sensorineural hearing loss (Table).[11,12]

We present the first reported fetal imaging of arrest of fetal brain development in a patient with postnatal diagnosis of ALG11-CDG. This report shows the development of microcephaly in ALG11-CDG during the late second and third trimester and with a phenotype consistent with arrest of fetal brain development or fetal brain disruption sequence.

Patient Description

A 30-year-old primigravida woman had a normal fetal anatomy obstetrical ultrasound (US) at 20 weeks' gestation, with fetal head circumference (HC) and biparietal diameter (BPD) both at the seventy-fifth percentile for gestational age. Specifically, the cavum septum pellucidum was visualized and the lateral cerebral ventricles had a normal configuration with a measurement of 6 mm at the level of the atria. At 36 0/7 weeks' gestation she had a follow-up obstetrical US because of lower than expected fundal height, which found microcephaly. She was referred to a maternal fetal medicine specialist, who by US described a male fetus in breech presentation with HC measuring 303 mm (consistent with 33 1/7 weeks) and BPD measuring 76 mm (consistent with 30 4/7 weeks), both measurements less than third percentile for gestational age. She was then referred to a fetal medicine center for fetal magnetic resonance imaging (MRI) and fetal neurology consultation.

Fetal US at (36 0/7 weeks) showed severe microcephaly, moderate lateral ventriculomegaly, redundant soft tissue around the occipital cranium, amniotic fluid index of 8, with an estimated fetal weight at the thirty-ninth percentile for gestational age. HC (282 mm, consistent with 30 6/7 weeks) and BPD (75 mm, consistent with 30 0/7 weeks) were less than first percentile for gestational age. Fetal MRI revealed severe cortical hypoplasia with a simplified gyral pattern, under rotated left hippocampus, moderate lateral ventriculomegaly measuring 14 mm in diameter at the level of the atria, complete agenesis of the corpus callosum, a collapse of the posterior occipital skull (Fig 1). The posterior fossa structures and the brainstem were of normal configuration; however, measurements of the transverse cerebellar diameter and height of the vermis were smaller than expected for age. No other body abnormalities were described by MRI or US.

The parents are Caucasian and are nonconsanguineous. There was no family history of neurological abnormalities or significant childhood illnesses. The couple had no recent travel to areas of endemic transmission of Zika virus. Maternal cytomegalovirus IgM and IgG and Zika virus IgM and polymerase chain reaction were negative at 36-weeks' gestation.

The infant boy was born via Caesarean section due to oligohydramnios and breech presentation at 37 1/7 weeks' gestation. Birth weight was 2879 g and HC was 32 cm (less than first percentile). Apgar scores were 9 and 9 at one and five minutes, respectively. On examination, he was microcephalic, the anterior fontanel was open and flat, and there was a palpable bony protuberance at the back of his head. He had normal newborn reflexes and no abnormal activity. Hearing screen was abnormal in both ears. He was breast-fed and was discharged home at age three days. Outpatient neurology examination at age three days described a microcephalic infant with a flat and short forehead, a bony prominence at the occiput, and a small anterior fontanel (Fig 1). There was redundant skin over the scalp and at the back of the neck. He was awake, had normal eye movements without nystagmus, pupils were equal and reactive to light, he had a normal suck and gag reflex, full facial movements, full strength with symmetric movements, some slip through and draping over on vertical and horizontal suspension, normal muscle stretch reflexes in upper and lower extremities, extensor plantar response, no ankle clonus, and normal palmar and plantar grasp reflex. He also had downslanting palpebral fissures, anteverted nares, low set ears with prominent lobes, and inverted nipples.

Postnatal brain MRI at age 16 days (3.5 weeks after the fetal MRI) showed microcephaly with cerebral hypoplasia, a simplified gyral pattern, agenesis of the corpus callosum, and no apparent growth of the cerebrum since the fetal MRI study (Fig 1). The ventral pons and cerebellar vermis, although normally formed, were smaller than expected for gestational age. The MRI also showed thin bands of decreased T1/T2 relaxation in the deep parietal and frontal white matter, extending into the subcortical regions, which may represent failed migration of neuronal elements.

At age three weeks he had periods of fussiness accompanied by breath-holding episodes (Table). The events were brief and self-resolved. An electroencephalogram was not performed at that time. At age six weeks he had increasing irritability with feeding. A fluoroscopy swallow study showed dysfunctional and delayed swallowing with esophageal reflux and silent aspiration so he was transitioned to full nasogastric tube feedings. He also had intermittent episodes of periodic breathing and poor control of body temperature.

Genetic testing

Chromosomal microarray was negative. Trio whole exome sequencing found compound heterozygous variants in trans in *ALG11*; one variant was maternally inherited (NM_001004127.2:c.44G>C/p.Arg15Thr) and one variant paternally inherited (c.161C>T/p.Ser54Leu). Both variants are exceedingly rare, with an allele frequency for the former of 14/276,856 alleles, whereas the latter allele is not present in gnomAD. No other variants potentially associated with the phenotype had been reported. The R15T variant occurs at a position that is conserved in mammals, and *in silico* analysis predicted this variant is probably damaging to the protein structure; however, the S54L substitution occurs at a position that is not conserved, and *in silico* algorithms were inconsistent as to whether the variant is damaging to the protein. Thus additional information was needed to validate the impact of these variants on protein glycosylation. Analysis of serum transferrin glycosylation status and total serum N-glycan analysis are often used, but these broad biomarkers were both normal. Western blot analysis of ALG11 protein in patient fibroblasts was also normal.

Validation required direct functional analyses on patient fibroblasts in a research laboratory. The first step was to examine hypoglycosylation of the cellular biomarker, GP130.[16] The second step was a determination of the size of the lipid-linked oligosaccharide (LLO) precursor of N-glycans.[11] Functional mutations in *ALG11* are predicted to generate a truncated LLO. In patient cells, GP130 was clearly underglycosylated and truncated LLO consistent with impaired ALG11 activity was also detected confirming the impact of the variant on protein glycosylation (Fig 2A-C).[17,18]

Discussion

We describe a patient with arrest of fetal brain development in a pregnancy with prior normal fetal biometry, for an infant found to have ALG11-CDG. Given the phenotype of skull collapse with occipital bone prominence and significant simplification of the gyral pattern seen at 36 weeks, the suspected onset of the arrested fetal

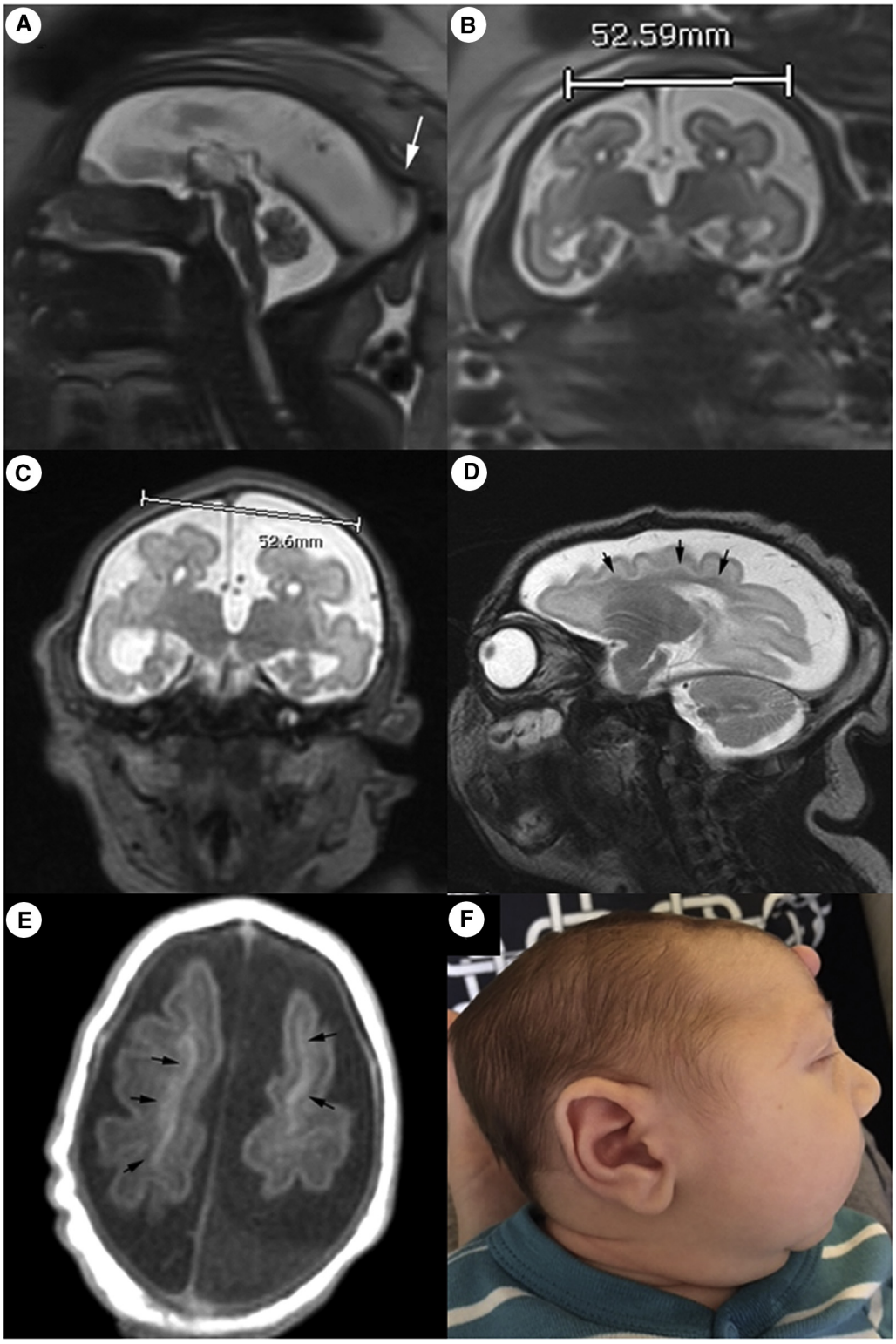

FIGURE 1. Clinical imaging of patient with ALG11-CDG. (A) Sagittal single shot fast spin-echo (SSFSE) T2-weighted image through the midline, fetus (36 weeks' gestational age). The skull is severely microcephalic, with a posterior shelf at the level of the lambdoid suture, characteristic of fetal brain disruption sequence. (B) Coronal SSFSE T2, fetus. The corpus callosum is absent. The cerebral hemispheres appear severely hypoplastic; the cerebral biparietal diameter is approximately 53 mm (expected range for normal fetus of 25 to 26 weeks' gestational age).[15] (C) Coronal fast spin-echo (FSE) T2 image at postnatal age 16 days (3.5 weeks after fetal MRI). The cerebrum has a similar configuration to the fetal image (B), except for mild interval enlargement of temporal horns. The cerebral biparietal diameter is unchanged at approximately 53 mm, reflecting a complete lack of growth of the cerebrum since the fetal MRI. The sagittal diameters of the cerebrum were also unchanged (not shown). (D) Sagittal FSE T2 through the right cerebral hemisphere neonate. A band tissue with low T2 signal tissue (arrows) is evident between the subcortical white matter and in the lining of the lateral ventricle, consistent with neuronal elements of the germinal matrix that have failed to migrate. (E) Axial spin-echo T1 through the upper cerebral hemispheres, neonate. A band of mildly increased T1 signal is evident deep to the subcortical white matter bilaterally (arrows), which corresponds to the band of low T2 signal noted on the sagittal image (D), consistent with neuronal elements that have failed to migrate. A slightly hyperintense subdural collection is evident behind the left cerebral hemisphere. (F) Profile photograph of infant at age 2 weeks showing microcephaly, posterior skull protuberance, and scalp rugae. CDG, congenital disorders of glycosylation; MRI, magnetic resonance imaging. The color version of this figure is available in the online edition.

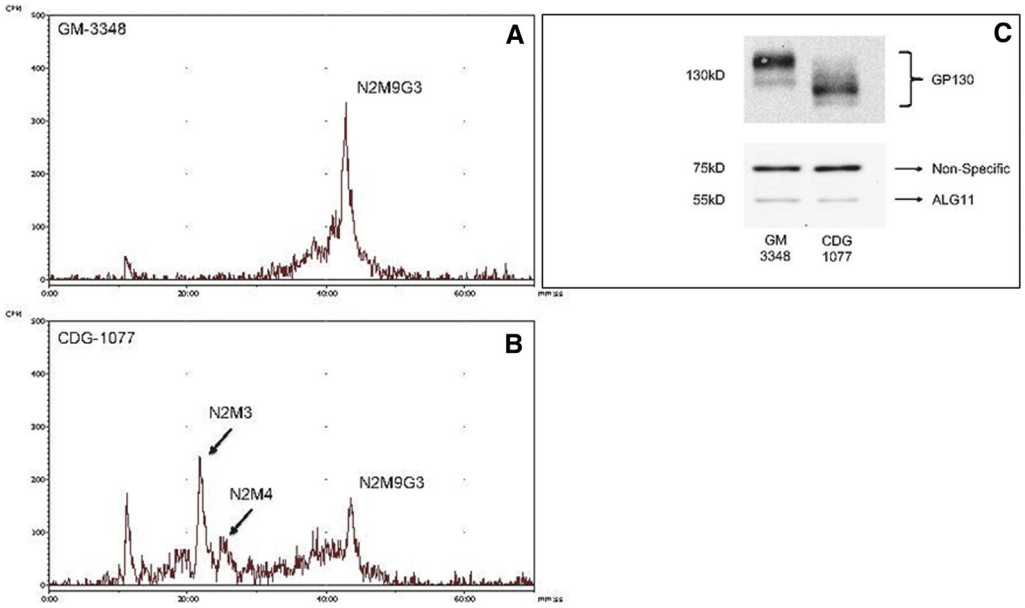

Figure 2. LLO and Western blot. LLO (A-B): Decreased $Glc_3Man_9GlcNAc_2$-PP-dolichol and increased $Man_3GlcNAc_2$-PP-dolichol and $Man_4GlcNAc_2$-PP-dolichol in patient (B, CDG-1077) as compared with control (A, GM-3348), indicating a block in the addition of the fourth and fifth mannoses to the LLO—reactions catalyzed by ALG11 [GlcNAc (N), mannose (M), glucose (G)]. (C) Western blot + GP130: ALG11 protein expression was unaltered. Hypoglycosylation of GP130 was detected in fibroblasts from the patient as judged by sodium dodecyl sulfate polyacrylamide gel electrophoresis migration detected by Western blot. Control = GM3348; patient = CDG1077. CDG, congenital disorders of glycosylation; LLO, lipid-linked oligosaccharide. The color version of this figure is available in the online edition.

brain development was during the latter part of the second trimester, around 28 weeks' gestation. The end of the second trimester coincides with a time of expansion of the volume of the cerebral cortex and increasing complexity of the cortical folding pattern. The failure of this occurrence in this patient with ALG11-CDG is also supported by the MRI findings of thin bands of decreased T1/T2 relaxation in the deep parietal and frontal white matter, which may represent disrupted neuronal cells. The additional finding of agenesis of the corpus callosum indicates a severe disruption of brain development. During the 3.5-week interval from the fetal MRI to the postnatal brain MRI, the brain did not increase in size, indicating an arrested growth pattern. This finding should be differentiated from a decrease in size, or atrophy, which did not occur during that same time period. It is not known how a deficiency of ALG11 activity caused an arrest of fetal brain development at this particular stage, although it can be postulated that the mutation disrupted cellular maturation of immature oligodendrocytes resulting in an arrest of brain growth at this particular stage. No additional postnatal neuroimaging was performed in this case. Other reported cases of ALG11-CDG report findings of cerebral atrophy (i.e., low cerebral volume compared with normative values) and microcephaly (Table),[11,12] and based on our case we anticipate that the other cases similarly have an arrested growth pattern.

Although the cerebellar volume was low for gestational age in our case, it was normally formed, and the low measurement was felt to be secondary to reduced cerebral volume rather than primary hypoplasia. Cerebellar atrophy with significant loss of Purkinje and granular cells appears to be a prominent neurological feature and has been found by neuropathology in PMM2-CDG (formerly CDG 1a).[19] Although cerebellar atrophy is usually found by postnatal imaging in PMM2-CDG, a prenatal diagnosis has been reported from cordocentesis at 27 weeks' gestation in a fetus with nonimmune hydrops.[20] Cerebellar atrophy to the extent seen in PMM2-CDG does not seem to be a consistent neuroimaging feature of ALG11-CDG (Table).

The skull finding associated with arrest of fetal brain development has been seen in other suspected autosomal recessive genetic conditions. Abdel-Salam et al.[4] reported four patients with severe microcephaly and developmental impairment in consanguineous families with this skull finding; however, a precise genetic mutation was not identified. Similar cases likely with potential genetic origin were reported by Moore et al.,[2] with varying degrees of cerebral destruction. The phenotype of skull collapse with occipital bone prominence is infrequently seen in cases of congenital microcephaly likely because of most genetic conditions causing a more slowly progressive reduction in fetal brain growth trajectory. This child may have a more severe phenotype of microcephaly in ALG11-CDG since the onset of microcephaly was before birth, whereas other reported cases of ALG11-CDG have a postnatal presentation of microcephaly (Table).[10-14]

Our patient presented at the height of the Zika virus epidemic and despite the absence of an epidemiologic link for Zika infection in the mother, Zika testing was performed and was negative. In cases of microcephaly from congenital Zika syndrome an irregular skull contour, similar to that seen in our case, could be detected even before 26 weeks' gestation.[21] Brain abnormalities in congenital Zika virus infection are often more destructive and associated with cortical dysplasia and polymicrogyria, which is not a feature of ALG11-CDG. Thus given the similarity in the brain findings with congenital Zika syndrome, genetic etiologies should be considered even if there is an epidemiologic link to Zika virus infection in the absence of positive maternal and newborn testing.

Interestingly, serum N-glycan analysis and carbohydrate-deficient transferrin were normal, but the novel GP130 biomarker revealed cellular hypoglycosylation, whereas LLO analysis was consistent with ALG11-CDG. It is important to note that a normal screening test via carbohydrate-deficient transferrin does not rule out an N-linked CDG, and in fact even the most common form of the disease, *PMM2*-CDG, can be associated with a normal serum result.[22,23]

Conclusions

The finding of severe microcephaly, scalp rugae, occipital bone prominence with skull collapse is in line with the description by Russell et al.[1] of fetal brain disruption sequence, which has not

previously been shown to occur in a CDG. ALG11-CDG should therefore be considered in the differential diagnosis of this infrequent skull finding in a patient with severe microcephaly.

Acknowledgement

The authors thank the patient and his family for their kind cooperation. H.H.F. is supported by the Rocket Fund and National Institutes of Health (NIH) grant R01DK99551. S.B.M wrote the first draft of the manuscript. There was no honorarium, grant, or other form of payment to S.B.M or any of the coauthors to produce the manuscript.

References

1. Russell LJ, Weaver DD, Bull MJ, Weinbaum M. In utero brain destruction resulting in collapse of the fetal skull, microcephaly, scalp rugae, and neurologic impairment: the fetal brain disruption sequence. Am J Med Genet. 1984;17:509–521.
2. Moore CA, Weaver DD, Bull MJ. Fetal brain disruption sequence. J Pediatr. 1990;116:383–386.
3. de Souza AS, de Oliveira-Szjenfeld PS, de Oliveira Melo AS, de Souza LAM, Batista AGM, Tovar-Moll F. Imaging findings in congenital Zika virus infection syndrome: an update. Childs Nerv Syst. 2018;34:85–93.
4. Abdel-Salam GMH, Abdel-Hamid MS, El-Khayat HA, et al. Fetal brain disruption sequence versus fetal brain arrest: a distinct autosomal recessive developmental brain malformation phenotype. Am J Med Genet A. 2015;167A:1089–1099.
5. Jaeken J. Congenital disorders of glycosylation. Handb Clin Neurol. 2013;113:1737–1743.
6. Ferreira CR, Altassan R, Marques-Da-Silva D, Francisco R, Jaeken J, Morava E. Recognizable phenotypes in CDG. J Inherit Metab Dis. 2018;41:541–553.
7. Freeze HH, Eklund EA, Ng BG, Patterson MC. Neurology of inherited glycosylation disorders. Lancet Neurol. 2012;11:453–466.
8. Fiumara A, Barone R, Del Campo G, Striano P, Jaeken J. Electroclinical features of early-onset epileptic encephalopathies in congenital disorders of glycosylation (CDGs). JIMD Rep. 2016;27:93–99.
9. O'Reilly MK, Zhang G, Imperiali B. In vitro evidence for the dual function of Alg2 and Alg11: essential mannosyltransferases in N-linked glycoprotein biosynthesis. Biochemistry. 2006;45:9593–9603.
10. Rind N, Schmeiser V, Thiel C, et al. A severe human metabolic disease caused by deficiency of the endoplasmatic mannosyltransferase hALG11 leads to congenital disorder of glycosylation-Ip. Hum Mol Genet. 2010;19:1413–1424.
11. Thiel C, Rind N, Popovici D, et al. Improved diagnostics lead to identification of three new patients with congenital disorder of glycosylation-Ip. Hum Mutat. 2012;33:485–487.
12. Regal L, van Hasselt PM, Foulquier F, et al. ALG11-CDG: three novel mutations and further characterization of the phenotype. Mol Genet Metab Rep. 2015;2:16–19.
13. Al Teneiji A, Bruun TU, Sidky S, et al. Phenotypic and genotypic spectrum of congenital disorders of glycosylation type I and type II. Mol Genet Metab. 2017;120:235–242.
14. Pereira AG, Bahi-Buisson N, Barnerias C, et al. Epileptic spasms in congenital disorders of glycosylation. Epileptic Disord. 2017;19:15–23.
15. Kline-Fath BM, Bulas DI, Bahado-Singh R. Fundamental and Advanced Fetal Imaging: Ultrasound and MRI. Wolters Kluwer; 2015.
16. Chan B, Clasquin M, Smolen GA, et al. A mouse model of a human congenital disorder of glycosylation caused by loss of PMM2. Hum Mol Genet. 2016;25:2182–2193.
17. Lacey JM, Bergen HR, Magera MJ, Naylor S, O'Brien JF. Rapid determination of transferrin isoforms by immunoaffinity liquid chromatography and electrospray mass spectrometry. Clin Chem. 2001;47:513–518.
18. Xia B, Zhang W, Li X, et al. Serum N-glycan and O-glycan analysis by mass spectrometry for diagnosis of congenital disorders of glycosylation. Anal Biochem. 2013;442:178–185.
19. Aronica E, van Kempen AA, van der Heide M, et al. Congenital disorder of glycosylation type Ia: a clinicopathological report of a newborn infant with cerebellar pathology. Acta Neuropathol. 2005;109:433–442.
20. Edwards M, McKenzie F, O'Callaghan S, et al. Prenatal diagnosis of congenital disorder of glycosylation type Ia (CDG-Ia) by cordocentesis and transferrin isoelectric focussing of serum of a 27-week fetus with non-immune hydrops. Prenat Diagn. 2006;26:985–988.
21. Sohan K, Cyrus CA. Ultrasonographic observations of the fetal brain in the first 100 pregnant women with Zika virus infection in Trinidad and Tobago. Int J Gynaecol Obstet. 2017;139:278–283.
22. Fletcher JM, Matthijs G, Jaeken J, Van Schaftingen E, Nelson PV. Carbohydrate-deficient glycoprotein syndrome: beyond the screen. J Inherit Metab Dis. 2000;23:396–398.
23. Hahn SH, Minnich SJ, O'Brien JF. Stabilization of hypoglycosylation in a patient with congenital disorder of glycosylation type Ia. J Inherit Metab Dis. 2006;29:235–237.